

1 Article

2 Temporal distribution measurement of the 3 parametric spectral gain in a photonic crystal fiber 4 pumped by a chirped pulse

5 Coralie Fourcade-Dutin ^{1,*}, Antonio Imperio ¹, Romain Dauliat ², Raphael Jamier ², Hector
6 Muñoz-Marco ³, Pere Pérez-Millán ³, Hervé Maillotte ¹, Philippe Roy ² and Damien Bigourd ¹

7

8 ¹ Institut FEMTO-ST, Département d'Optique, UMR 6174 CNRS-Université Bourgogne Franche-Comté,
9 25030 Besançon, France; c.fourcadedutin@femto-st.fr

10 ² Université Limoges, CNRS, XLIM, UMR 7252, F-87000 Limoges; philippe.roy@xlim.fr

11 ³ FYLA LASER SL, Ronda Guglielmo Marconi 12, 46980, Paterna (Valencia), Spain

12

13 * Correspondence: c.fourcadedutin@femto-st.fr;

14

15 Received: date; Accepted: date; Published: date

16 **Abstract:** The temporal distribution of the spectral parametric gain is experimentally investigated
17 when a chirped pump pulse is injected in a photonic crystal fiber. A pump-probe experiment was
18 developed and the important characteristics was measured as the chirp of the pump, the signal
19 pulse and the gain of the parametric amplifier. We highlight that the amplified spectrum depends
20 strongly on the instantaneous pump wavelength and that the temporal evolution of the wavelength
21 at maximum gain is not monotonic. This behavior is significantly different from the case in which
22 the chirped pump has a constant peak power. This measurement will be very important to
23 efficiently include parametric amplifiers in laser systems delivering ultra-short pulses.

24 **Keywords:** Parametric amplification; Four wave mixing; Fiber Optics

25

26

27 1. Introduction

28 Ultra-fast optical parametric amplification (OPA) has already demonstrated many interesting
29 features for the amplification of ultra-short pulses. It allows to get a very high gain value and a very
30 large gain bandwidth to amplify pulses with a duration as short as few optical cycles [1]. In addition,
31 as the parametric process is based on an instantaneous nonlinearity, this type of amplification is of
32 prime interest to maintain or enhance the temporal contrast [2,3]. Most of the OPA based ultra-fast
33 sources are developed with nonlinear crystals as the amplifier media and they are often reliable
34 enough for most of applications [4]. Alternatively, ultra-fast four wave mixing in an optical fiber is a
35 promising direction toward the OPA of ultra-short pulses at high gain in a compact and rugged
36 geometry [5,6]. In this case, the ultra-short signal has a very large bandwidth and is firstly stretched
37 before the amplification to decrease the peak power and to limit spurious nonlinearities in the fiber.
38 After the amplification, the signal is recompressed close to its initial pulse duration. The strong pump
39 pulse has a relatively long duration (tens of ps to ns) to match the one of the stretched signal [5, 7-9].
40 More recently, several configurations of fiber based OPA have been performed to amplify a very
41 large spectral width at high gain [10-13] or a narrower band at high energy in the μJ range [14-16]. In
42 particular, we have shown that ultra-broad band parametric amplification at high gain can be
43 obtained by using a single pump stretched pulse with a relatively broad spectrum [10-11]. In this

44 case, the spectral parametric gain is distributed in the temporal domain since the instantaneous
 45 frequency of the pump changes quasi-linearly with time due to the chirp rate. Therefore, we can
 46 expect to amplify a stretched ultra-short pulse when a broad band signal is simultaneously injected
 47 in the optical fiber [12]. However, the instantaneous frequencies of the stretched signal also change
 48 with time and they need to match the temporal distribution of the spectral gain. In addition, the
 49 temporal shape of the pump impacts strongly the parametric gain shape since the gain value and/or
 50 the phase matching condition depend both on the instantaneous power injected in the fiber [16,17] or
 51 in a nonlinear crystal [18]. Therefore, it is very important to measure and understand the temporal
 52 distribution of this spectral gain in order to design ultra-broad band parametric amplifiers. This
 53 feature cannot be measured with a spectrometer that record a time integrated spectrum. Hence, in
 54 this manuscript, we present a pump-probe method with stretched pulses to diagnose this
 55 distribution. The paper is structured as follow. In Section 2, we present didactic examples to highlight
 56 the temporal evolution of the spectral gain when the pump power is not constant during its duration.
 57 In Section 3, we describe the experimental set-up. The most important properties was measured as
 58 the chirp of the pump, the signal pulse and the parametric fluorescence. The measurement of the
 59 parametric gain as a function of the delay between the pump and the probe is discussed in Section 4.
 60 We highlight that the amplified spectrum depends strongly on the instantaneous pump wavelength
 61 and that the temporal evolution of the wavelength at maximum gain is not monotonic. Finally, we
 62 conclude the article in Section 5.

63 2. Parametric amplification in fiber pumped by a structured and chirped pump pulse

64 Parametric amplification in fiber of an ultra-short pulse relies on a phase matched four wave mixing
 65 of a stretched signal with a very large bandwidth, a strong pump pulse with a power P and a
 66 generated idler. In this manuscript, the pump will be a chirped pulse. The gain of the signal is
 67 maximum when all the involved waves are phase matched according to

$$68 \quad \kappa(\Omega, t) = \beta_{20} \cdot \Omega^2 + \frac{\beta_{40}}{12} \cdot \Omega^4 + 2\gamma P(\tau) = 0 \quad (1)$$

69 with β_{20} and β_{40} the second and fourth order dispersion terms at the pump wavelength λ_p . We neglect
 70 higher order terms. Ω is the angular frequency offset from the pump. γ is the nonlinear coefficient of
 71 the fiber and is set to $35 \text{ W}^{-1} \cdot \text{km}^{-1}$. In order to calculate the phase matching condition (Eq. 1), we
 72 consider the photonic crystal fiber (PCF) used in the experiment. From the input facet of the PCF
 73 measured with a scanning electron microscope (inset in Figure 1.a), the second order dispersion term

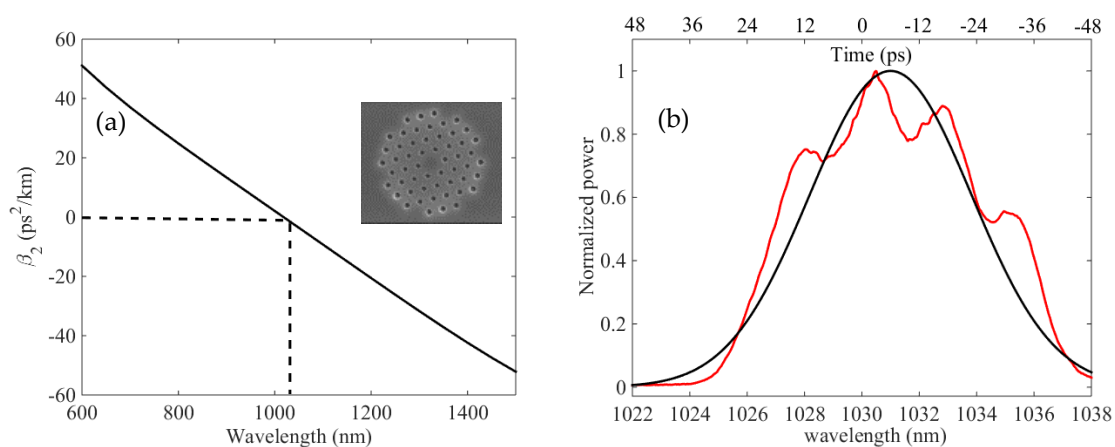
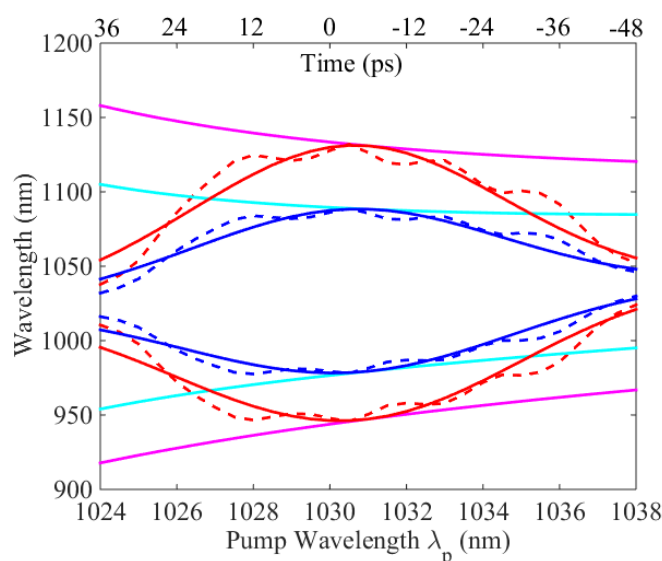


Figure 1. (a) Second order dispersion term as the function of the wavelength. Inset. Input facet of the PCF measured with a scanning electron microscope. (b) Normalized pump spectrum of a chirped pulse with a Gaussian shape (black line) or with the experimental profile (red line).

74 as the function of the wavelength is calculated (Figure 1.a). The SEM image is first, turned into a two-
 75 color image that represents the refractive index map. A mesh is then created from this index map and
 76 both, effective indices and intensity distributions of electric and magnetic fields are then calculated
 77 using a commercial mode solver based on the finite element method. The chromatic dispersion curve
 78 is simply deduced from the effective index one leading to the determination of the zero dispersion
 79 wavelength (ZDW) at 1020 nm.

80 For comparison, we firstly calculated the phase matching condition as a function of λ_p for a constant
 81 peak power of 600 W (Figure 2, magenta solid lines) and 200 W (Figure 2, cyan solid lines). In both
 82 cases, the phase matched wavelengths evolve monotonically with λ_p . Since we aim to investigate the
 83 impact of the pulse shape of a chirped pump, the instantaneous power P will be time dependent in
 84 the following. For example, the spectral profile of the pump originated from an ultra-fast laser has
 85 usually a Gaussian profile. In our configuration, the pulse is stretched with a linear chirp rate
 86 $\alpha = \tau / (\lambda_p - \lambda_{p0})$ with λ_{p0} the pump central wavelength. Therefore, the temporal profile has also a
 87 Gaussian profile. Figure 1.b (black line) displays a spectrum centered at $\lambda_{p0} = 1031$ nm with a
 88 bandwidth equals to 6 nm at Full Width at Half Maximum (FWHM). The full pump spectrum lies in
 89 the anomalous dispersion regime of the PCF. For $\alpha = 6$ ps/nm close to the experimental value, the pulse
 90 duration is 36 ps. Figure 2 shows the phase matching condition calculated from Eq. 1 for the Gaussian
 91 pump profile with a maximum power of 600 W (red solid line) and 200 W (blue solid line) at 1030
 92 nm.

93



94

95 **Figure 2.** Phase matching as a function of the pump wavelength for a chirped pulse with a Gaussian spectrum
 96 (solid red and blue lines) or with the experimental profile (dashed red and blue lines). The maximum power is
 97 600 W (red lines) or 200 W (blue lines). The magenta and cyan lines correspond to the phase matching for a
 98 constant peak power of 600 W or 200 W, respectively.

99 In these cases, the curves are not monotonic and have Bell shapes with a maximum and a minimum
 100 at 1131/946 nm (for 600 W) and 1088/978 nm (200 W) at $\lambda_p \sim 1031$ nm. As a result, the phase matched
 101 wavelength can be obtained at two different λ_p . For example, the parametric amplification at 1100 nm
 102 can occur at $\lambda_p \sim 1027$ nm and $\lambda_p \sim 1034$ nm. For the chirped pump pulse owing a linear temporal
 103 distribution of λ_p , it also means that the amplification at 1100 nm can be obtained at two times delayed
 104 by 43.4 ps. When a signal is injected in the PCF simultaneously with the chirped pump, its
 105 amplification is considerably affected by the pump shape. For a CW signal [15], two delayed
 106 amplifications occur and therefore, two idler pulses are generated during the parametric process.

107 Alternatively, if a chirped seed with a broad bandwidth is injected in the FOPA [12], the parametric
 108 process will reshape the amplified signal and it depends strongly on the delay between the signal
 109 and the pump. In addition, any variation of the pump profile will modify the phase matching
 110 condition. In our experiment, the pump spectrum is modulated (Figure 1.b, red line) impacting also
 111 the phase matching condition (Figure 2, dashed lines). It is worth noting that Figure 2 takes into
 112 account only the parametric process in the strong pump regime. The saturation and the Raman
 113 process are not included although it may modify the amplification behavior. Therefore, it is highly
 114 important to directly measure the temporal distribution of the spectral gain in the experimental
 115 conditions.

116

117 3. Experimental set-up and main parameters

118 3.1. Pump-probe set-up

119 The experimental setup is displayed in Figure 3. The pump and the signal are both generated from a
 120 unique mode-locked oscillator (Flint, LightConversion) delivering a train of pulses at 76 MHz with a
 121 duration of 80 fs at FWHM centered at 1030 nm. The total average power is 1.5 W. The pump
 122 wavelength is set at 1030 nm while the signal one should be tunable to seed the targeted parametric
 123 amplification band. In order to shift the signal spectrum, a beam splitter selects a part of the oscillator
 124 output and 400 mW are injected in an all normal dispersion fiber (ANDI) to generate a coherent
 125 continuum [19]. It extends from ~750 nm to 1250 nm and therefore it can be used to seed a parametric
 126 amplifier in this band. Then, the continuum is injected in a Öffner type stretcher. The selection of the
 127 signal wavelength is achieved by the stretcher alignment by rotating the grating. The spectral
 128 bandwidth is imposed by the finite size of the mirrors in the stretcher. The other part of the oscillator
 129 (around 750 mW) seeds the pump amplifier. It is composed of a volume Bragg grating (VBG) that
 130 stretched the pulses to a duration of few tens of ps. The chirped pulse is then injected in an
 131 acousto-optic modulator (AOM) to decrease the repetition rate to 1 MHz and amplified by two
 132 ytterbium doped fiber amplifiers (YDFA). The maximum average power is 1 W. Finally, the pump
 133 and the signal are both injected in the 5 meter long PCF. The properties of the PCF was described in
 134 Section 2. The two pulses are synchronized with a delay stage and the amplification spectrum is
 135 measured with an optical spectrum analyzer (OSA) for several delays. As the signal is shorter than
 136 the pump pulse, the instantaneous gain is measured for a selected part of the pump.

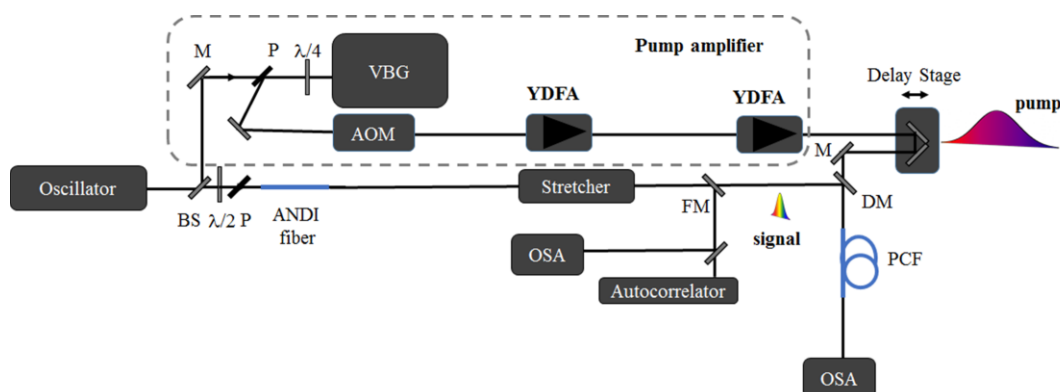


Figure 3. Experimental set-up. VBG, volume Bragg grating; AOM, acousto-optic modulator; YDFA, ytterbium doped fiber amplifier; OSA, optical spectrum analyser; PCF, photonic crystal fiber; ANDI, all normal dispersion fiber; BS, beam splitter; M, mirror; P, polarizer; DM, dichroic mirror; FM, flipped mirror;

137 The spectrum at the PCF output was firstly measured with the OSA for an average pump power of
 138 31 mW, when the signal was not injected (Figure 4.a). It shows two lobes at 992 nm and 1077 nm

139 together with the pump spectrum at 1030 nm. The bandwidth at 1077 nm is ~12 nm. The experimental
 140 pump spectrum is shown in Figure 1.b (red line) and exhibits structures due to self phase modulation
 141 (SPM) occurring in the last YDFA. Therefore, we expect that this spectral modulation will impact the
 142 temporal distribution of the spectral gain. In the next section, the signal will be injected in the PCF
 143 together with the chirped pump pulse. Therefore, the continuum (black line in Figure. 4.b) is filtered
 144 in the stretcher to select the signal spectrum at 1080 nm (red line in Figure. 4.b) close to the central
 145 value of the lobes (Figure 4.a). The spectral bandwidth is 15 nm (FWHM). The duration of the
 146 stretched pulse was measured with an autocorrelator and the experimental trace is shown in Figure
 147 4.c (red points). From a Gaussian fit (solid black line in Figure 4.c), we deduce a pulse duration of 4.2
 148 ps. This pulse duration is a good compromise since several constraints need to be considered. Indeed,
 149 a very short pulse allows to get a high temporal resolution in the pump-probe measurement.

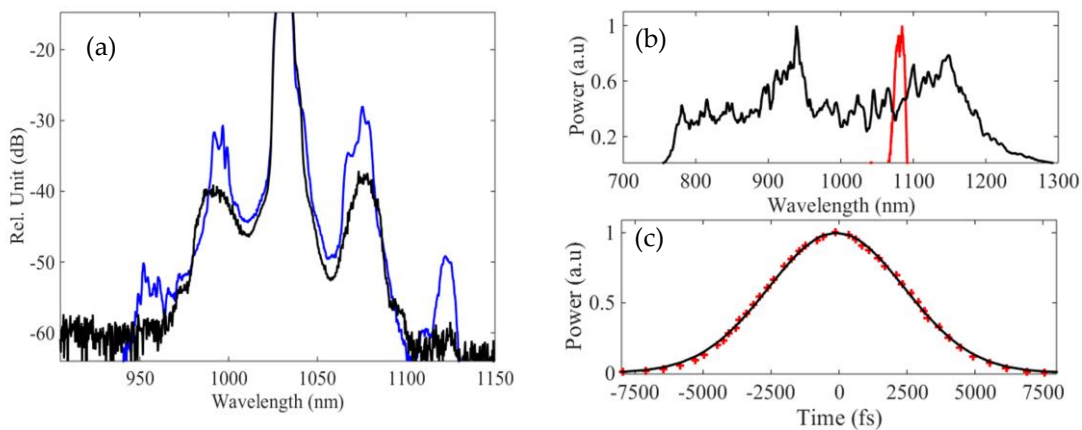


Figure 4. (a) Fluorescence spectrum when the PCF is pumped by 31 mW (black line). Output spectrum when the signal is injected at null delay (blue line). (b) Spectrum of the continuum generated in the ANDI fiber (black line) and spectrum of the signal (red line). (c) Autocorrelation trace (red stars) and the Gaussian fit (solid black

150 However, in this case, the signal pulse can produce SPM even for a low power. For a longer pulse
 151 duration, the chirp from the stretcher should also be taken into account in the gain analysis since the
 152 signal wavelength will be distributed in the temporal domain. In our case, we assume that the signal
 153 chirp is negligible compared to the one of the pump since the signal duration is shorter by a factor
 154 >10.

155
 156 *3.2. Characterization of the pump*

157
 158 For each delay between the long chirped pump and the short probe, the signal (the probe) overlaps
 159 with one slide of the pump owing an instantaneous power and wavelength. Therefore, it is highly
 160 important to measure the temporal distribution of the pump wavelength. We measured the chirp
 161 rate, **corresponding to the spectral phase**, by spectral interferometry between a long and a short
 162 pulse both at the pump wavelength [20]. Accordingly, we modified the set-up. Briefly, a part of the
 163 output of the amplifier was injected at the opposite side of the VBG to recompress it to ~300 fs. Then,
 164 the chirped pump and the compressed pulse was combined with a beam splitter and the interference
 165 pattern was recorded with the OSA. Due to the finite resolution of the spectrometer, the complete
 166 interference pattern cannot be measured over the full spectrum. Therefore, a local fringe can be
 167 measured directly at the null delay between the two pulses. For more details, we refer the reader to
 168 the reference [21] describing the method. For example, the inset in Figure 5.a displays an example of
 169 the interference pattern occurring at 1030 nm. In order to get the chirp rate, the spectral location of the
 170 fringe was measured as a function of the delay between the long and short pulses (Figure 5.a). The
 171 null delay is fixed at 1030 nm. From a linear fit, we deduced a α value of 6.2 ps/nm; i.e the pump
 172 wavelengths evolves linearly with time. Combining this value with the spectrum (Figure 1), the

173 temporal shape can be inferred (Figure 5.b). The pulse duration is 55 ps (FWHM) and the temporal
 174 shape is modulated with a period of ~14 ps.
 175

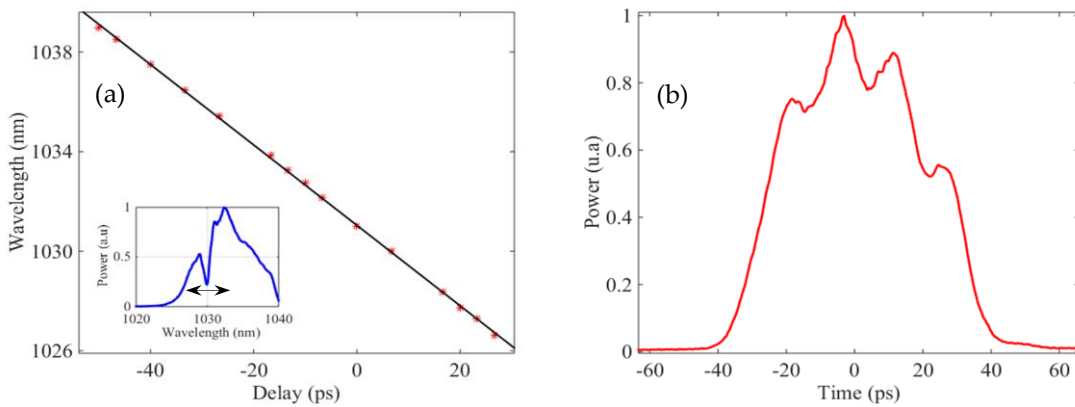


Figure 5. (a) Measurement of the chirp rate by spectral interferometry and its linear fit leading to $\alpha=6.2$ ps/nm. The inset is an example of the interference pattern. (b) Temporal shape of the pump pulse.

176 **4. Measurement of the amplification and discussion**

177 To measure the instantaneous gain, the chirped pump pulse is injected in the PCF simultaneously
 178 with the signal. The delay $\Delta\tau$ between the two pulses is tuned and the amplified spectrum is recorded
 179 for every delay separated by 3.3 ps. **To ensure that the pump power launched in the PCF is constant**
 180 **during the complete measurement, we checked that the fluorescence spectrum is identical for each**
 181 **delay.** The amplification has been measured between $\Delta\tau \sim -15$ and $+25$ ps. For longer delay, we have
 182 not detected any clear amplification since the pump power is lower by almost 50 % from its
 183 maximum. From the pump average power and the pulse duration (Figure 5.b), the peak power is
 184 estimated at ~ 530 W. The signal average power is ~ 5 μ W. Figure 4.a (blue line) shows an example of
 185 an output spectrum when the signal is injected at $\Delta\tau$ around 0 ps. An idler is generated confirming
 186 the amplification of the signal. We can also observe some other bands at 952 and 1124 nm resulting
 187 from cascaded four wave mixings. Figure 6.a and Figure 6.b show a selection of amplified and idler
 188 spectra when the $\Delta\tau$ is tuned from -6.6 ps to +19.8 ps.
 189

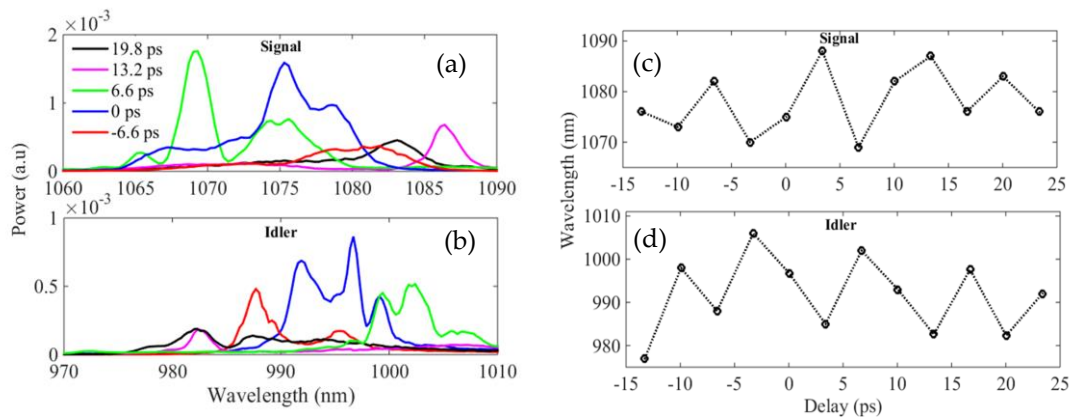
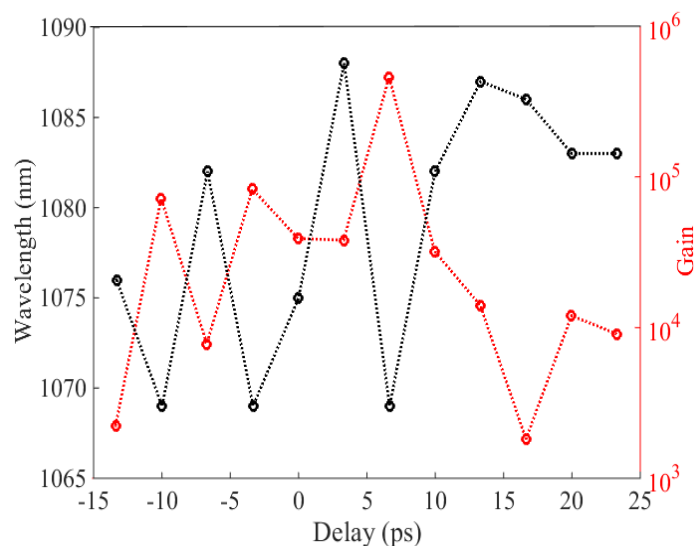


Figure 6. (a-b) Selection of amplified and idler spectra when the delay is tuned from -6.6 ps to +19.8 ps. (c-d) Variation of the signal and idler wavelengths at the maximum amplification as a function of the delay.

201
 202
 203
 204
 205
 206
 207
 208
 209
 210
 211
 212
 213
 214
 215
 216
 217
 218
 219
 220
 221
 222
 223
 224
 225
 226
 227
 228
 229
 230

The null delay corresponds to the pump wavelength of 1030 nm (Figure 5). However, we cannot accurately define it and we set it when the amplification is maximum near the center of the signal spectrum (blue line in Figure 6.a). For each $\Delta\tau$, the amplification clearly occurs at a selected wavelength. In addition, the amplified shapes and their bandwidths vary with $\Delta\tau$ since the signal pulse overlaps with a different portion signal of the pump. Therefore, the pump power and the dispersion at the pump wavelength change with the delay and influence the properties of the amplified signal as explained in Section 2. Particularly, the pump temporal shape is modulated around $\Delta\tau = 0$ ps and has a Bell shape (Figure 5.b). Therefore the variation of the wavelengths at the maximum amplification with $\Delta\tau$ (Figure 6.b) is not monotonic and is modulated. The amplification of one given signal wavelength can be achieved at several delays. This behavior is significantly different from the case in which the chirped pump has a constant peak power since only the dispersion parameter changes with time. In this case, the wavelength at maximum amplification evolves monotonically [11].

We also calculated the gain from the spectra of the input and the amplified signal. We remind that the repetition rate of the signal is 76 MHz while the pump one is 1 MHz. Thus, it needs to be taken into account in the gain measurement; the output/input ratio at the signal wavelength does not give directly the net gain of amplification. Indeed, the instantaneous amplification occurs when the pump and the signal temporally overlap while the OSA detects the average power of all the incoming pulses. Therefore, the net gain is derived from $G = S_{amp} / S_{in} \cdot 76$ with S_{amp} and S_{in} the amplified and input signal spectra at the PCF output. Figure 7 displays the evolution of the wavelength at maximum gain as a function of $\Delta\tau$ (black circles) and it shows a similar behavior as in Figure 6.b. For each delay, the maximum gain is very high (red circles in Figure 7) and it ranges from 1.8×10^3 to 4.6×10^5 for signal wavelength extending from ~ 1068 to ~ 1088 nm. We checked that the amplifier does not saturate since the gain does not change when the input power of the signal was decreased by a factor 10. In addition, no spectral broadening of the signal by SPM was observed since the amplified spectra was not significantly different at lower power. **Similarly, the measurement of the saturated gain cannot be measured directly since the increase of the signal input power will create SPM.**



231
 232
 233
 234
 235
 236
 237

Figure 7. Maximum gain value (red circles) and its corresponding signal wavelength (black circles) as a function of the delay.

238 5. Conclusions

239 We presented a pump-probe experiment enabling the characterization of the temporal distribution
240 of the spectral gain in a fiber based optical parametric amplifier pumped by a chirped pump. We
241 showed that the gain value and the amplified spectrum varies importantly when the signal overlaps
242 with a different portion of the pump pulse. This measurement will be very important to include
243 efficiently the fiber based OPA in a laser system delivering ultra-short pulses. For example, when a
244 chirped signal is injected in the PCF with the chirped pump pulse, the temporal evolution of the
245 signal wavelength should match closely the distribution of the spectral gain measured with our
246 method.

247

248 **Author Contributions:** CFD, AI and DB conceived, designed and performed the full experiment; AI and CFD
249 analyzed the data; RD, HMM and PPM designed the PCF; RD and RJ achieved the PCF modeling; RD, PR, HMM
250 and PPM fabricated the PCF and RJ, HMM and PPM characterized it. CFD, PR, HM and DB supervised the
251 project (PCF, experiment and simulation) and contributed to experimental tools and concepts. CFD and DB
252 wrote the manuscript.

253

254 **Funding:** This research was funded by the ANR, grant number FiberAmp/ANR-16-CE24-0009, the EUR EIPHI
255 program (ANR-17-EURE-0002), the Franche-Comté councils (SIMULIE and CORPS project).

256

257 **Conflicts of Interest:** “The authors declare no conflict of interest.”

258

259 References

- 260 1. Ciriolo A. G.; Negro M.; Devetta M.; Cinquanta E.; Facciala D.; Pusala A.; De Silvestri S.; Stagira S.; Vozzi
261 C. Optical Parametric Amplification Techniques for the Generation of High-Energy Few-Optical-Cycles IR
262 Pulses for Strong Field Applications. *Appl. Sci.* **2017**, *7*, 265-293
- 263 2. Bigourd D.; Patankar S.; Olsson Robbie S. I.; Doyle H. W.; Mecseki K.; Stuart N.; Hadjicosti K.; Leblanc N.;
264 New G. H. C.; Smith. R. A. Spectral enhancement in optical parametric amplifiers in the saturated
265 regime. *Appl. Phys. B* **2013**, *113*, 627-633
- 266 3. Dorrer C.; Begishev I. A.; Okishev A.V.; Zuegel J.D. High-contrast optical parametric amplifier as a front
267 end of high-power laser systems. *Opt. Lett.* **2007**, *32*, 2143-2145
- 268 4. Fu Y.; Yuan H.; Midorikawa K.; Lan P.; Takahashi E.J. Towards GW-scale isolated attosecond pulse far
269 beyond carbon K-Edge driven by mid-infrared waveform synthesizer. *Appl. Sc.* **2018**, *8*, 2451
- 270 5. Hanna M., Druon F., Georges P. Fiber optical parametric chirped-pulse amplification in the femtosecond
271 regime. *Opt. Express* **2006**, *14*, 2783-2790
- 272 6. Faccio D.; Grün A.; Bates P.K; Chalus O.; Biegert J. Optical amplification in the near-infrared in gas filled
273 hollow-core fibers. *Opt. Lett.* **2009**, *34*, 2918-2920
- 274 7. Cristofori V., Lali-Dastjerdi V., Rishj L. S., Galili M., Peucheretand C., Rottwitt K. Dynamic characterization
275 and amplification of sub-picosecond pulses in fiber optical parametric chirped pulse amplifiers. *Opt.*
276 *Express* **2013**, *21*, 26044-26051
- 277 8. Caucheteur C., Bigourd D., Hugonnot E., Szriftgiser E., Kudlinski A., Gonzalez-Herraez M., Mussot A.
278 Experimental demonstration of optical parametric chirped pulse amplification in optical fiber. *Opt. Lett.*
279 **2010**, *35*, 1786-1788
- 280 9. Bigourd D.; Lago L.; Mussot A.; Kudlinski A.; Gleyze J.F.; Hugonnot E. High-gain, optical-parametric,
281 chirped-pulse amplification of femtosecond pulses at 1 μm . *Opt. Lett.* **2010**, *20*, 3480-3482
- 282 10. Bigourd D.; Beauré d’Augères P.; Dubertrand J.; Hugonnot E.; Mussot A. Ultra-broadband fiber optical
283 parametric amplifier pumped by chirped pulses. *Opt. Lett.* **2014**, *39*, 3782-3785
- 284 11. Vanvincq O.; Fourcade-Dutin C.; Mussot A.; Hugonnot E.; Bigourd D. Ultrabroadband fiber optical
285 parametric amplifiers pumped by chirped pulses. Part 1: analytical model. *J. Opt. Soc. Am. B* **2015**, *32*, 1479-
286 1487

- 287 12. Fourcade-Dutin C.; Vanvincq O.; Mussot A.; Hugonnot E.; Bigourd D. Ultrabroadband fiber optical
288 parametric amplifiers pumped by chirped pulses. Part 2: sub-30 fs pulse amplification at high gain. *J. Opt.*
289 *Soc. Am. B* **2015**, *32*, 1488-1493
- 290 13. Bigourd D.; Fourcade-Dutin C.; Vanvincq O.; Hugonnot E. Numerical analysis of broadband fiber optical
291 parametric amplifiers pumped by two chirped pulses. *J. Opt. Soc. Am. B* **2016**, *33*, 1800-1807
- 292 14. Morin P.; Dubertrand J.; Beauré d'Augères P.; Quiquempois Y.; Bouwmans G.; Mussot A.; Hugonnot E. μ J-
293 level Raman-assisted fiber optical fiber parametric chirped pulse amplification. *Opt. Lett.* **2018**, *43*, 4683-
294 4686
- 295 15. Fu W.; Wise F. W. Normal-dispersion fiber optical parametric chirped-pulse amplification. *Opt. Lett.* **2018**,
296 *43*, 5331-5334
- 297 16. Bigourd D.; Morin P.; Dubertrand J., Fourcade-Dutin C.; Maillotte H., Quiquempois Y.; Bouwmans G.,
298 Hugonnot E. Parametric gain shaping from a structured pump pulse. *IEEE Phot. Techno. Lett.* **2019**, *31*,
299 214-217
- 300 17. Finot C.; Wabnitz S. Influence of the pump shape on the modulation instability process induced in a
301 dispersion-oscillating fiber. *J. Opt. Soc. Am. B* **2015**, *32*, 892-899
- 302 18. Lee H. W.; Kim Y. G.; Yoo J.Y.; Yoon J.W.; Yang J. M.; Lim H.; Nam C.H.; Sung S.H.; Lee S.K. Spectral
303 shaping of an OPCPA preamplifier for a sub-20 fs multi-PW laser. *Opt. Express* **2018**, *26*, 24775-24783
- 304 19. Fourcade-Dutin C. ; Bigourd D. Near infrared tunable source delivering ultra-short pulses based on an all
305 normal dispersion fiber and a zero dispersion line. *Appl. Phys. B*, **2018**, *124*, 154
- 306 20. Kovacs A.P.; Osvay K.; Kurdi G.; Gorde M.; Klebniczki J.; Bor Z. Dispersion control of a pulse stretcher-
307 compressor system with two-dimensional spectral interferometry. *Appl. Phys. B*, **2005**, *80*, 165-170
- 308 21. Dou T.H; Tautz R ; Gu X. ;Marcus G. ; Feurer T. ; Krausz F. ; Veisz L. Dispersion control with reflection
309 gratings of an ultra-broadband spectrum approaching a full octave. *Opt. Express* **2010**, *18*, 27900-27909
- 310
311



© 2019 by the authors. Submitted for possible open access publication under the terms and conditions of the Creative Commons Attribution (CC BY) license (<http://creativecommons.org/licenses/by/4.0/>).

312
313
314
315
316
317
318
319